Journal of Solid Mechanics Vol. 6, No. 2 (2014) pp. 150-157

New Approach to Instability Threshold of a Simply Supported Rayleigh Shaft

M. Faraji Mahyari[1,*], KH. Faraji Mahyari[1], S. Fardpour[2]

[1]*Department of Mechanical Engineering, Islamic Azad University, Shahr-e Rey Branch, 7th Km, Khalij Fars highway, 3319118751, Tehran, Iran*
[2]*Department of Industrial Design, Islamic Azad University, Shahr-e Rey Branch, 7th Km, Khalij Fars highway, 3319118751, Tehran, Iran*

Received 17 February 2014; accepted 4 April 2014

ABSTRACT

The main goal of this research is to analyse the effect of angular velocity on stability and vibration of a simply supported Rayleigh rotating shaft. To this end, non-dimensional kinetic and potential energies are written while lateral vibration is considered. Finite element method is employed to discrete the formulations and Linear method is applied to analyse instability threshold of a rotating shaft. These results represent the significant effects of mass moment of inertia, centrifugal forces and rotational speed. Also, the differences between Rayleigh and Euler-Bernoulli modelling are delivered. Furthermore, the effect of slenderness ratio on instability threshold and the natural frequencies are illustrated. Increasing rotational speed leads to decreasing of instability threshold and forward and backward natural frequencies. These formulations can be used to choose the safe working conditions for a shaft.

© 2014 IAU, Arak Branch.All rights reserved.

Keywords: Rayleigh rotating shaft; Stability; Vibration; Forward and backward natural frequencies

1 INTRODUCTION

ROTATING shaft is one of the most commonly employed mechanical elements for power transmission such as drill strings and gas turbines. Vibrations occur in rotating machinery due to centrifugal force, gyroscopic effect, unbalance mass, external forces and power transmission. Many researches analyze vibration and instability threshold of rotating shafts.

Grybos [1] considered the effect of shear deformation and rotary inertia of a rotor on its critical speeds. Choi et al. [2] presented the consistent derivation of a set of governing differential equations describing the flexural and the torsional vibrations of a rotating shaft while a constant compressive axial load was acted on it. Jei and Leh [3] investigated the whirl speeds and mode shapes of a uniform asymmetrical Rayleigh shaft with asymmetrical rigid disks and isotropic bearings. Singh and Gupta [4] studied Free damped flexural vibrations analysis of composite cylindrical tubes using beam and shell theories. Kang and Tan [5] studied transverse waves propagating in an infinitely long rotating Timoshenko shaft subjected to axial forces and the effects of rotation speed, axial force and axial deformation are found. Delivered model included the contributions of axial deformation to the transverse vibration of the rotating shaft. Jun and Kim [6] studied free bending vibration of a rotating shaft composed of multi-step segments. In this research, shaft is modeled as a Timoshenko beam and gyroscopic effect and torque applied at

* Corresponding author. Tel.: +98 939 445 3359.
E-mail address: farajimahyari@iausr.ac.ir (M. Faraji Mahyari).

© 2014 IAU, Arak Branch. All rights reserved.

each part of the shaft are considered. Mohiuddin and Khulief [7] represented a finite element formulation of the dynamic model for a rotor-bearing system. In this research, the elastodynamic model of coupled bending and torsional motions of the rotating shaft is derived and gyroscopic effects and the inertia coupling between bending and torsional deformations are considered. Gu and Cheng [8] studied the dynamic response of a high-speed spindle subject to a moving mass while shaft is modelled as a high-speed rotating shaft using Timoshenko beam theory and the effects of mass moving speed, the Rayleigh coefficient and the mass ratio are discussed. Behzad and Bastami [9] investigated the effect of shaft rotation on its natural frequency. In this model, natural frequencies are studied while the gyroscopic effect, axial force originated from centrifugal force and Poisson effect are considered. Banerjee and Su [10] developed dynamic stiffness matrix of a spinning composite beam to investigate its free vibration characteristics including bending–torsion coupling effect. Hosseini and Khadem [11] studied free vibrations of an in-extensional simply supported rotating shaft with nonlinear curvature and inertia. In this research rotary inertia and gyroscopic effects are included, but shear deformation is neglected and the method of multiple scales is used to analyze free vibrations of the shaft.

In previous research, the effects of moment of inertia and centrifugal force weren't considered as an important factor on instability threshold and forward and backward natural frequencies of a Rayleigh shaft. So the main idea of this research is to analyze instability threshold and forward and backward natural frequencies of a Rayleigh shaft while the effects of centrifugal force, shaft moment inertia, gyroscopic effect and bending deformation by Euler-Bernoulli theory are considered. In this model, Rayleigh shaft is used because the results represent the significant effects of centrifugal force produced by moment of inertia. In Euler-Bernoulli shaft, moment of inertia isn't considered and the formulation cannot detect instability threshold of the shaft. Also considering large slenderness ratio, shear deformation's effect is neglected.

In this research, considering lateral and axial vibration, kinetic and potential energies of an element of a Rayleigh rotating shaft are derived. In kinetic energy, translational and rotational energy, gyroscopic and centrifugal effects are considered and a constant rotational speed is assumed. In potential energy, the bending deformation is considered. Then, finite element method is employed to discrete the integral energy equations and the global matrixes are assembled. Then using Lagrange formula, the vibration equations are obtained. Considering static instability and dropping time dependent terms in vibration equations, instability threshold equations are obtained. Solution of these equation leads to equilibrium position and its instability can be found by examining the sign of second order derivative of energy equations. Results represent the significant effects of moment of inertia and centrifugal terms on forward and backward frequencies and instability threshold, so they cannot be neglected. Also the effects of slenderness ratio on forward and backward natural frequencies and instability threshold are delivered.

2 FORMULATION

Referring to Fig.1, the kinetic and potential energies of an element of a shaft in a rotating coordinate (with constant angular velocity Ω about x axis) can be written as (Yigit and Christoforou, [12] and [13]):

$$U_e = \frac{1}{2}\int_{x_e}^{x_e+L_e}\left(EI_{ez}\left(v''\right)^2 + EI_{ey}\left(w''\right)^2\right)dx \tag{1}$$

$$T_e = \frac{1}{2}\rho A_e\int_{x_e}^{x_e+L_e}\left(\dot{v}^2+\dot{w}^2\right)dx + \frac{1}{2}\int_{x_e}^{x_e+L_e}\left(J_{ey}\left(\dot{w}'+\Omega v'\right)^2 + J_{ez}\left(\dot{v}'-\Omega w'\right)^2\right)dx \tag{2}$$

Eq. (1) represents bending potential energy of a shaft's element. In this equation, v and w are the shaft's deflections in y and z (lateral) directions respectively, E is the Young's modulus of elasticity, I_e is the area moment of inertia, x_e is the global coordinate of the first node of element, I_e is the length of element and $(\ )'$ denotes partial derivative with respect to x. Also, index e refers to element. Eq.(2) represents the kinetic energy of a shaft's element which produced by lateral vibrations. In this equation, ρ_s is the density, Ω is the shaft angular velocity, J_e is mass moment of inertia and $(\dot{\ })$ denotes partial derivative with respect to time (t).

Using the following variables, the energy equations can be converted to a non-dimensional form.

© 2014 IAU, Arak Branch

$$v = \bar{v}L, w = \bar{w}L, t = \delta_t \tau, \bar{\Omega} = \delta_t \Omega, x = \xi L_e, \delta_t = \sqrt{\frac{\rho A L^4}{E I_y \gamma_t^4}}, \delta_D = \frac{D}{L}, x_1 = \bar{x}_1 L, L_e = L\bar{L}_e \tag{3}$$

For simplicity, in the following equations the sign $\bar{}$ aren't written in non-dimensional variables.

$$v(x,t) = [\phi(x)]\{v(t)\}_e = [\phi_1(\xi) \quad \phi_2(\xi) \quad \phi_3(\xi) \quad \phi_4(\xi)]\{v_1(t) \quad \theta_{w1}(t) \quad v_2(t) \quad \theta_{w2}(t)\}^T \tag{4}$$

$$w(x,t) = [\varphi(x)]\{w(t)\}_e = [\varphi_1(\xi) \quad \varphi_2(\xi) \quad \varphi_3(\xi) \quad \varphi_4(\xi)]\{w_1(t) \quad \theta_{v1}(t) \quad w_2(t) \quad \theta_{v2}(t)\}^T \tag{5}$$

Using finite element method and beam's shape functions, integral equations of energies are converted to scalar ones. Beam's shape functions delivered in Eqs. (4) and (5). In these relations, the variables v_i, w_i, θ_{vi} and θ_{wi} are the displacement and slope of the element's nodes, and indexes 1 and 2 refer to the element's nodes numbers. Also $\phi_i(\xi)$ and $\varphi_i(\xi)$ refer to shape functions of the beam element which represented in the following equations.

$$\begin{aligned} &\phi_1(\xi) = \varphi_1(\xi) = 1 - 3\xi^2 + 2\xi^3 && \phi_2(\xi) = -\varphi_2(\xi) = L_e\left(\xi - 2\xi^2 + \xi^3\right) \\ &\phi_3(\xi) = \varphi_3(\xi) = 3\xi^2 - 2\xi^3 && \phi_4(\xi) = -\varphi_4(\xi) = L_e\left(-\xi^2 + \xi^3\right) \\ &\xi = \frac{x - x_1}{L_e}, \quad x_1 \le x \le x_2, \quad x_2 = x_1 + L_e \end{aligned} \tag{6}$$

In Eq. (6), ξ is the local coordinate of the element and x_1 and x_2 are the global coordinates of the first and second nodes of the element, respectively. Also L_e is the length of the element. These parameters are delivered in Fig.1.

Substituting Eqs.(4) and (5) into non-dimensional energy equations and integrating, leads to following equations:

$$U_e = \frac{1}{2}\{v\}_e^T \left[K^{vv}\right]_e \{v\}_e + \frac{1}{2}\{w\}_e^T \left[K^{ww}\right]_e \{w\}_e \tag{7}$$

$$\begin{aligned} T_e = &\frac{1}{2}\Omega^2 \{v\}_e^T \left[M^{vvJy\Omega}\right]_e \{v\}_e + \frac{1}{2}\Omega^2 \{w\}_e^T \left[M^{wwJz\Omega}\right]_e \{w\}_e + \Omega\{\dot{w}\}_e^T \left[M^{wvJy\Omega}\right]_e \{v\}_e \\ &-\Omega\{\dot{v}\}_e^T \left[M^{vwJz\Omega}\right]_e \{w\}_e + \frac{1}{2}\{\dot{w}\}_e^T \left(\left[M^{ww}\right]_e + \left[M^{wwJy}\right]_e\right)\{\dot{w}\}_e + \frac{1}{2}\{\dot{v}\}_e^T \left(\left[M^{vv}\right]_e + \left[M^{vvJz}\right]_e\right)\{\dot{v}\}_e \end{aligned} \tag{8}$$

For simplicity to find the effect of angular velocity, the parameter Ω is written outside of kinetic energy matrices. In discrete kinetic energy equation, phrases have coefficient Ω are known as gyroscopic terms and the ones have coefficient Ω^2 are known as centrifugal terms. Because the formulations of the above matrices are too massive, they aren't represented here.

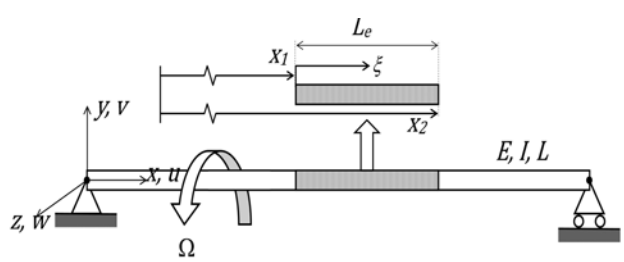

Fig. 1
The scheme of a rotating shaft.

© 2014 IAU, Arak Branch

3 TOTAL ENERGY EQUATIONS

The vectors and matrixes of elements are assembled to obtain the global ones. The notations of global vectors and matrixes are similar to the ones used for elements but the index e which represents "element", is dropped. To apply boundary conditions of simply supported beam, the lateral displacements of the first and last nodes are deleted.

The final forms of kinetic and potential energies are as follow:

$$\begin{aligned} T &= \frac{1}{2}\{\dot{v}\}^T\left(\left[M^{vv}\right]+\left[M^{vvJz}\right]\right)\{\dot{v}\}+\frac{1}{2}\Omega^2\{v\}^T\left[M^{vvJy\Omega}\right]\{v\}+\Omega\{\dot{w}\}^T\left[M^{wvJy\Omega}\right]\{v\} \\ &\frac{1}{2}\{\dot{w}\}^T\left(\left[M^{ww}\right]+\left[M^{wwJy}\right]\right)\{\dot{w}\}+\frac{1}{2}\Omega^2\{w\}^T\left[M^{wwJz\Omega}\right]\{w\}-\Omega\{\dot{v}\}^T\left[M^{vwJz\Omega}\right]\{w\} \end{aligned} \tag{9}$$

$$U_e = \frac{1}{2}\{v\}^T\left[K^{vv}\right]\{v\}+\frac{1}{2}\{w\}^T\left[K^{ww}\right]\{w\} \tag{10}$$

$$\begin{aligned} \{v\}^T &= \left\{\theta_{w1} \quad v_2 \quad \theta_{w2} \quad \cdots \quad v_n \quad \theta_{w(n)} \quad \theta_{w(n+1)}\right\}_{2n} = \left\{\bar{v}_1 \quad \bar{v}_2 \quad \ldots \quad \bar{v}_{2n-1} \quad \bar{v}_{2n}\right\} \\ \{w\}^T &= \left\{\theta_{v1} \quad w_2 \quad \theta_{v2} \quad \cdots \quad w_n \quad \theta_{v(n)} \quad \theta_{v(n+1)}\right\}_{2n} = \left\{\bar{w}_1 \quad \bar{w}_2 \quad \ldots \quad \bar{w}_{2n-1} \quad \bar{w}_{2n}\right\} \end{aligned} \tag{11}$$

4 EQUATIONS OF MOTIONS AND EQULIBRIUM POSITION

Equations of motions should be found to analyse vibration and instability threshold of the shaft. To this goal, the Lagrangian of the system is defined by Π as represented in Eq. (12) and the Lagrange formula (i.e Eq. (13)) is applied to it. The results are represented in Eqs. (14) and (15).

$$\Pi = T - U \tag{12}$$

$$\frac{d}{dt}\left(\frac{\partial \Pi}{\partial \dot{q}}\right)-\frac{\partial \Pi}{\partial q}=\{0\} \tag{13}$$

$$\left(\left[M^{vv}\right]+\left[M^{vvJz}\right]\right)\{\ddot{v}\}-\Omega^2\left[M^{vvJy\Omega}\right]\{v\}-\Omega\left[M^{wvJy\Omega}\right]\{\dot{w}\}-\Omega\left[M^{vwJz\Omega}\right]\{\dot{w}\}+\left[K^{vv}\right]\{v\}=\{0\} \tag{14}$$

$$\left(\left[M^{ww}\right]+\left[M^{wwJy}\right]\right)\{\ddot{w}\}-\Omega^2\left[M^{wwJz\Omega}\right]\{w\}+\Omega\left[M^{vwJz\Omega}\right]\{\dot{v}\}+\Omega\left[M^{wvJy\Omega}\right]\{\dot{v}\}+\left[K^{ww}\right]\{w\}=\{0\} \tag{15}$$

Eqs. (14) and (15) are the vibrational equations of a Rayleigh rotating shaft. In these equations, the phrases with Ω^2 coefficients are the centrifugal terms and the phrases with Ω, are the gyroscopic terms. In these equations, the centrifugal terms have negative sign, so they tend to decrease the stiffness and stability of the shaft. Using conventional methods, the forward and backward natural frequencies of the Rayleigh shaft can be found.

To analyse the instability, equilibrium positions of the shaft should be found and then, its instability should be examined. In this research, the static instability of shaft is investigated, so the time dependent terms can be dropped from energy equations (Timoshenko and Gere [14]) and static Lagrangian is formed as Eq. (16).

$$\Pi_s = \Pi\big|_{\dot{v}=0,\dot{w}=0} \tag{16}$$

Applying Lagrange formula to static Lagrangian, the equilibrium equations can be found (Timoshenko and Gere [14]). As a result, the ordinary differential equations are converted to algebraic equations such as those represented in the following equations:

$$\frac{\partial \Pi_s}{\partial \bar{v}_i} = \left(\left[K^{vv}\right]-\Omega^2\left[M^{vvJy\Omega}\right]\right)\{v\}=\{0\} \tag{17}$$

© 2014 IAU, Arak Branch

$$\frac{\partial \Pi_s}{\partial \overline{w}_i} = \left(\left[K^{ww}\right] - \Omega^2 \left[M^{wwJz\Omega}\right]\right)\{w\} = \{0\} \tag{18}$$

Solving the above equations concludes equilibrium positions (Timoshenko and Gere [14]) which is $\{v\}_E = \{w\}_E = \{0\}$. This results represent straight attitude of the shaft.

Now, examining the sign of second order derivative of the static Lagrangian, the stability of the equilibrium position can be found (Timoshenko and Gere [14]) as follow:

$$\left[\frac{\partial^2 \Pi_s}{\partial \overline{v}_i \partial \overline{v}_j}\right] = \left[K^{vv}\right] - \Omega^2 \left[M^{vvJy\Omega}\right] \tag{19}$$

$$\left[\frac{\partial^2 \Pi_s}{\partial \overline{w}_i \partial \overline{w}_j}\right] = \left[K^{ww}\right] - \Omega^2 \left[M^{wwJz\Omega}\right] \tag{20}$$

$$\left[\frac{\partial^2 \Pi_s}{\partial \overline{v}_i \partial \overline{w}_j}\right] = [0] \tag{21}$$

If the matrix of second order derivatives of the static Lagrangian is positive definite, the equilibrium position is stable, otherwise it is unstable (Timoshenko and Gere [14]; Hildebrand [15]). So the following relation is obtained for the shaft stability reshold:

$$\det\left(\begin{bmatrix} \left[\frac{\partial^2 \Pi_s}{\partial \overline{v}_i \partial \overline{v}_j}\right] & \left[\frac{\partial^2 \Pi_s}{\partial \overline{v}_i \partial \overline{w}_j}\right] \\ \left[\frac{\partial^2 \Pi_s}{\partial \overline{w}_i \partial \overline{v}_j}\right] & \left[\frac{\partial^2 \Pi_s}{\partial \overline{w}_i \partial \overline{w}_j}\right] \end{bmatrix}\right) > 0 \tag{22}$$

Eliminating zero matrices in Eq.(22) and considering symmetry of cross section which leads to the same matrices in v and w direction, the condition can be simplified as below:

$$\det\left[\frac{\partial^2 \Pi_s}{\partial \overline{v}_i \partial \overline{v}_j}\right] > 0 \quad or \quad \det\left[\frac{\partial^2 \Pi_s}{\partial \overline{w}_i \partial \overline{w}_j}\right] > 0 \tag{23}$$

Eq.(23) represents the instability threshold of the shaft. Substituting the parameters of the shaft in obtained conditions, its stability can be specified. If all Eigen values of the matrices in Eq. (23) (or Eq. (22)) are positive, the shaft is stable, otherwise, if at least one of the Eigen values is zero or negative, the shaft is unstable.

5 NUMERICAL RESULTS

The vibration and stability formulation developed above is applied to illustrative example to verify and represent results. The first set of results represents validation of formulation.

The forward and backward natural frequencies of a rotating shaft with simply supported ends are represented in the following equation (Rao, [16]).

© 2014 IAU, Arak Branch

$$\omega_n = \frac{r^2\lambda_n^2\Omega \pm \sqrt{\left(r^2\lambda_n^2\Omega\right)^2 + C_0\left(1+r^2\lambda_n^2\right)\lambda_n^4}}{1+r^2\lambda_n^2}, \quad r = \frac{D}{4}, \quad \lambda_n = \frac{n\pi}{L}, \quad C_0 = \sqrt{\frac{EI}{\rho A}} \tag{24}$$

Using vibrational equations (Eqs. (14) and (15)) and dropping centrifugal terms (terms with Ω^2), the obtained results for backward and forward natural frequencies are the same as Eq.(24).

Also, assigning $\Omega = 0$ in Eqs. (14) and (15), the obtained natural frequencies are the same as the natural frequencies of a simply supported beam.

Table 1
Data used in the modeling.

6 element used in modelling	$E = 2\times10^{11} N/m^2$
$\gamma_t = \pi$	$\rho = 7850 Kg/m^3$
$D = 10mm$	

The parameters delivered in Table 1. are used in following simulations. The first part of obtained results is delivered in Fig.2 for $\delta_{D1} = 15$. In this figure, first forward and backward natural frequencies of a shaft are delivered while centrifugal terms are considered and dropped. In this figure, the centrifugal terms are considered in $Cent.$ curves while they are neglected in $Gyr.$ curves. On the other hand, the $Cent.$ curves are obtained by Euler-Bernoulli model of the shaft, whereas $Gyr.$ curves are delivered by Rayleigh model. This figure shows that as the non-dimensional rotational speed increases, the difference between $Cent.$ and $Gyr.$ curves become large. This figure represents the significant effects of centrifugal terms which produced by the moment of inertia of a Rayleigh shaft, so these terms couldn't be neglected in the modelling of a rotating shaft.

It should be noted that without considering moment of inertia and centrifugal terms (i.e. Euler-Bernoulli assumption), the forward natural frequencies have an ascending curve. However, considering these effects (i.e. Rayleigh assumption) causes an ascending curve at first and a descending curve at the follow. These effects are produced by the negative sign of centrifugal terms which tend to reduce the stiffness of the shaft.

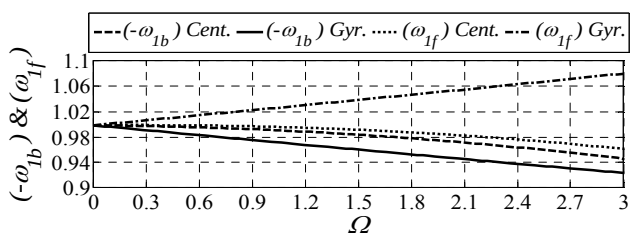

Fig. 2
First forward and backward natural frequencies by considering and dropping centrifugal terms for $\delta_{D1} = 15$.

The effects of non-dimensional rotational speed on the first and second forward and backward natural frequencies are delivered in Fig.3 and Fig.4 for $\delta_{D1} = 15$. As shown in these figures, both of natural frequencies decrease as the rotational speed increases and the first backward frequency vanishes at a specific rotational speed. This rotational speed is known as critical rotational speed (CRS) which causes shaft's instability. At CRS, the centrifugal force and moment of inertia of Rayleigh shaft overcome the stiffness of the shaft so the first backward natural frequency tens to zero. The CRS only can be detected for a Rayleigh rotating shaft and for an Euler-Bernoulli beam, this threshold cannot be achieved.

© 2014 IAU, Arak Branch

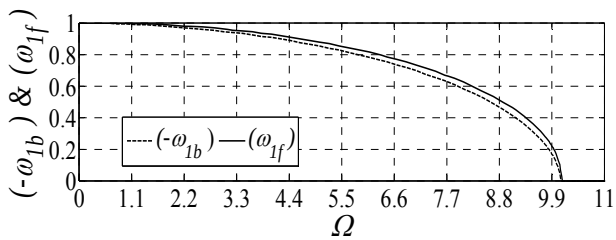

Fig. 3
The effects of non-dimensional rotational speed on the first forward and backward natural frequencies for $\delta_{D1} = 15$.

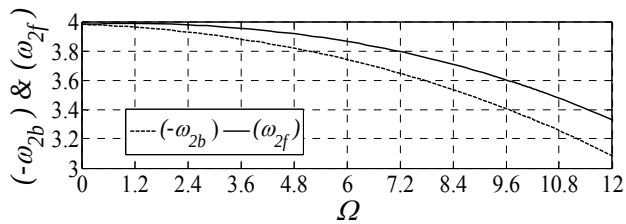

Fig. 4
The effects of non-dimensional rotational speed on the second forward and backward natural frequencies for $\delta_{D1} = 15$.

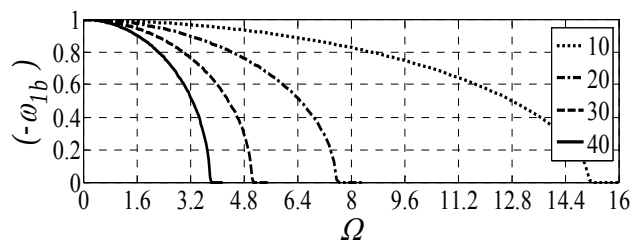

Fig. 5
The effect of rotational speed on first backward natural frequency of a shaft for different slenderness ratio.

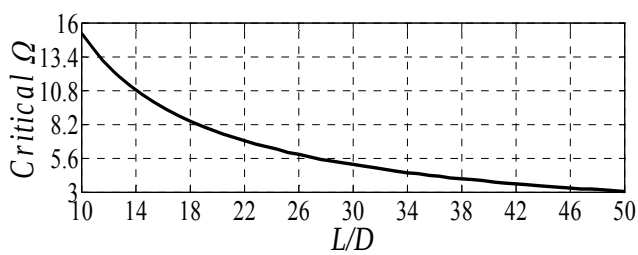

Fig. 6
The effect of slenderness ratio on CRS.

In the next step, the effects of rotational speed on first backward natural frequency of a Rayleigh rotating shaft are delivered in Fig.5 for different slenderness ratios. As shown in this figure, all backward natural frequencies decrease as rotational speed increases. Also in this figure, the effects of slenderness ratio on first backward natural frequency are represented. As the slenderness ratio increases, the non-dimensional first backward natural frequency decreases. Additionally, the effects of slenderness ratio on CRS are delivered in Fig.5, and CRS deceases as slenderness ratio increases. As shown in previous results, the CRS depends on parameters of the shaft such as slenderness ratio, so in the follow, the effect of slenderness ratio on CRS is delivered in Fig.6. As shown in this figure, CRS decreases as slenderness ratio increases and approach to the first natural frequency of a simply supported beam. This figure shows that as the slenderness ratio increases, centrifugal force and the effects of moment of inertia become large, so they cannot be neglected.

6 CONCLUSIONS

In this research, the effects of angular velocity on stability and vibration of a simply supported Rayleigh rotating shaft were analysed. To this end, non-dimensional kinetic and potential energies were written while lateral

© 2014 IAU, Arak Branch

vibrations were considered and finite element method was employed to discrete the formulations. Then linear stability method was applied to analyse instability threshold of a Rayleigh rotating shaft. In the follow, the significant effects of moment of inertia and centrifugal forces on the first and second forward and backward natural frequencies were delivered, so these effects couldn't be neglected. On the other hand, the results represented the differences between Euler-Bernoulli and Rayleigh shaft. Considering moment of inertia (Rayleigh shaft), the shaft might become unstable, however an Euler-Bernoulli model couldn't detect instability threshold. Also, increasing of the shaft slenderness ratio led to decreasing of the natural frequencies and critical rotational speed. These formulations can be used to choose the safe working conditions for a Rayleigh shaft. As future work, this formulation can be applied to different boundary conditions. Also this formulation can be mixed with an axially excited shaft to find unstable zone. Moreover, the shaft can be modelled by Timoshenko theory and the effects of shear deformation can be examined.

ACKNOWLEDGEMENTS

The authors gratefully acknowledge the financial and other support of this research (Whirling and buckling instability threshold of a slender rotor with geometrical variable axial force), provided by Islamic Azad University, Shahr-e Rey Branch, Tehran, Iran.

REFERENCES

[1] Grybos R., 1991, Effect of shear and rotary inertia of a rotor at its critical speeds, *Archive of Applied Mechanics* **61** (2): 104-109.

[2] Choi S.H., Pierre C., Ulsoy A. G., 1992, Consistent modelling of rotating timoshenko shafts subject to axial loads, *Journal of Vibration, Acoustics, Stress, and Reliability in Design* **114** (2):249-259.

[3] Jei Y. G., Leh C. W., 1992, Modal analysis of continuous asymmetrical rotor-bearing systems, *Journal of Sound and Vibration* **152** (2):245-262.

[4] Singh S. P., Gupta K., 1994, Free damped flexural vibration analysis of composite cylindrical tubes using beam and shell theories, *Journal of Sound and Vibration* **172** (2):171-190.

[5] Kang B., Tan C. A., 1998, Elastic wave motions in an axially strained, infinitely long rotating timoshenko shaft, *Journal of Sound and Vibration* **213**(3):467-482.

[6] Jun O. S., Kim J. O., 1999, Free bending vibration of a multi-step rotor, *Journal of Sound and Vibration* **224**(4):625-642.

[7] Mohiuddin M. A., Khulief Y. A., 1999, Coupled bending torsional vibration of rotors using finite element, *Journal of Sound and Vibration* **223**(2):297-316.

[8] Gu U. C., Cheng C. C., 2004, Vibration analysis of a high-speed spindle under the action of a moving mass, *Journal of Sound and Vibration* **278**:1131-1146.

[9] Behzad M., Bastami A. R., 2004, Effect of centrifugal force on natural frequency of lateral vibration of rotating shafts, *Journal of Sound and Vibration* **274**:985-995.

[10] Banerjee J. R., Su H., 2006, Dynamic stiffness formulation and free vibration analysis of a spinning composite beam, *Computers and Structures* **84**:1208-1214.

[11] Hosseini S.A., Khadem S. E., 2009, Free vibrations analysis of a rotating shaft with nonlinearities in curvature and inertia, *Mechanism and Machine Theory* **44**:272-288.

[12] Yigit A. S., Christoforou A. P., 1996, Coupled axial and transverse vibration of oil well drill string, *Journal of sound and vibration* **195** (4):617-627.

[13] Yigit A. S., Christoforou A. P., 1997, Dynamic modelling of rotating drill strings with borehole interactions, *Journal of sound and vibration* **206**(2):243-260.

[14] Timoshenko G., 1963, *Theory of Elastic Stability*, Mc Graw Hill, United state.

[15] Hildebrand F. B., 1984, *Methods of Applied Mathematics*, Prentice Hall Ind, United state.

[16] Rao J. S., 1983, *Rotor Dynamics*, New York, John Wiley & Sons, United state.

© 2014 IAU, Arak Branch